Supporting Information for Publication

Plasmonic Library Based on Substrate-Supported Gradiential Plasmonic Arrays

Mareen B. Müller,[†] Christian Kuttner,[†] Tobias A. F. König,[†,#] Vladimir V. Tsukruk,[#]

Stephan Förster,[§] Matthias Karg,[§] and Andreas Fery[†*]*

[†]Physical Chemistry II, University of Bayreuth, Universitätsstrasse 30, 95447 Bayreuth, Germany

[#]School of Materials Science and Engineering, Georgia Institute of Technology, Atlanta, Georgia 30332-0245, United States of America

[§]Physical Chemistry I, University of Bayreuth, Universitätsstrasse 30, 95447 Bayreuth, Germany

* andreas.fery@uni-bayreuth.de; * matthias.karg@uni-bayreuth.de

SI 1: UV-vis extinction spectra of gold cores and core/shell particles in aqueous solution

The optical properties of the gold cores prior to encapsulation and the core/shell hybrid particles were analyzed by UV-vis extinction spectroscopy (Figure S1). The black spectrum was measured for the gold cores before the polymer encapsulation. The position of the localized surface plasmon resonance is 518 nm. The red spectrum corresponds to the core/shell colloids. In comparison to the spectrum of the gold cores, the extinction for the core/shell particles shows a pronounced increase in extinction toward lower wavelength. This can be attributed to scattering from the rather large PNIPAM shell.[1] In addition the LSPR is slightly shifted to higher wavelength due to the increased refractive index, *i.e.*, PNIPAM has a higher refractive index than water.

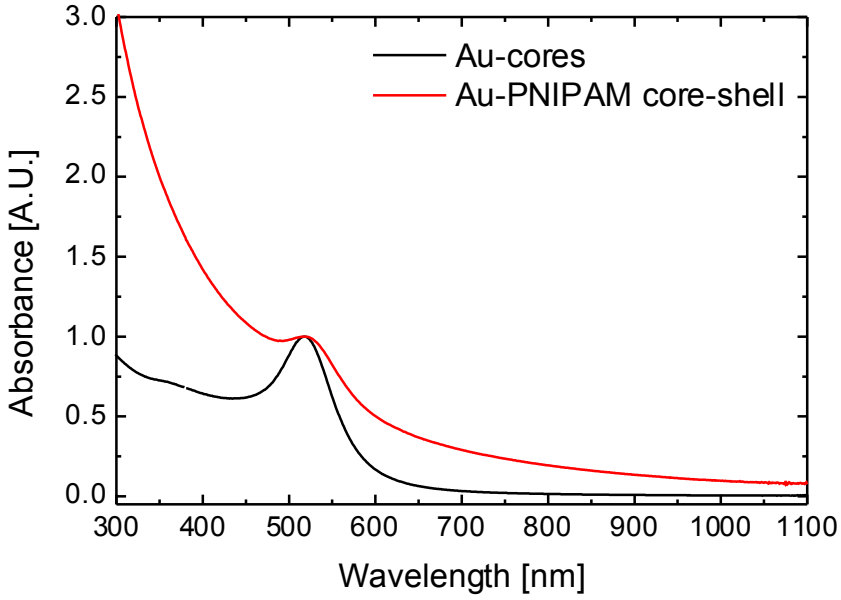

Figure S1: UV-vis extinction spectra of citrate stabilized gold (black line) and gold-core/PNIPAM-shell particles (red line) measured in water at 25 °C.

SI 2: AFM height profile of particle monolayer

Representative image of the spin-coated Au-core/PNIPAM-shell monolayer before overgrowth of the gold cores.

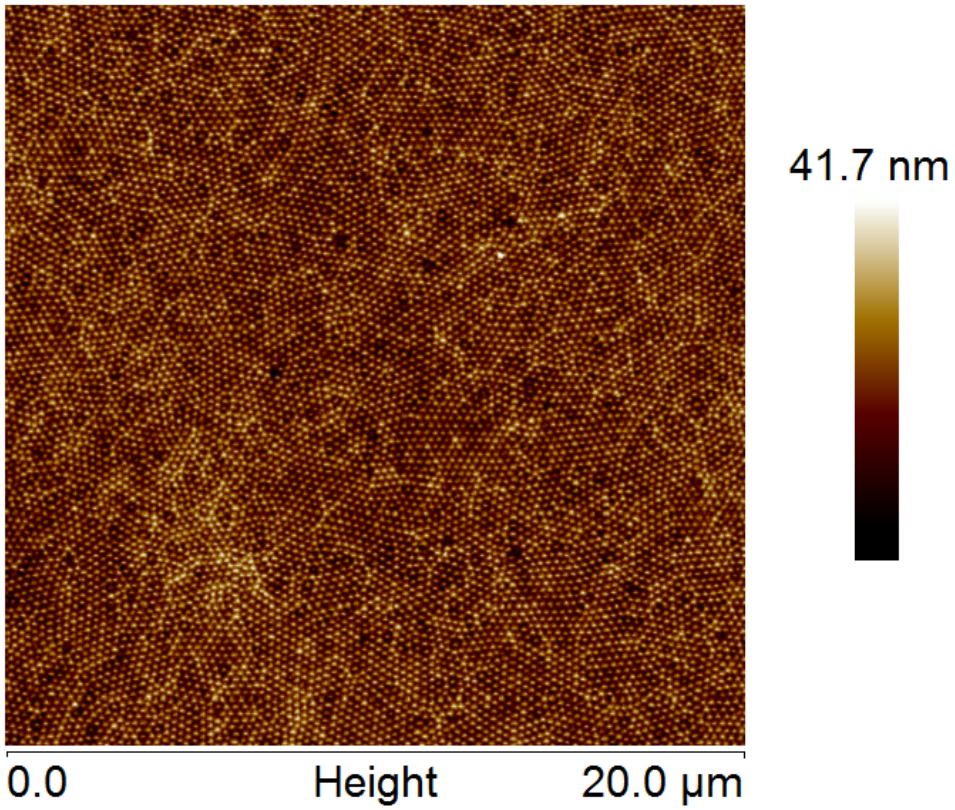

Figure S2: AFM height image of a representative Au-core/PNIPAM-shell monolayer after spin-coating.

SI 3: Details on withdrawal process

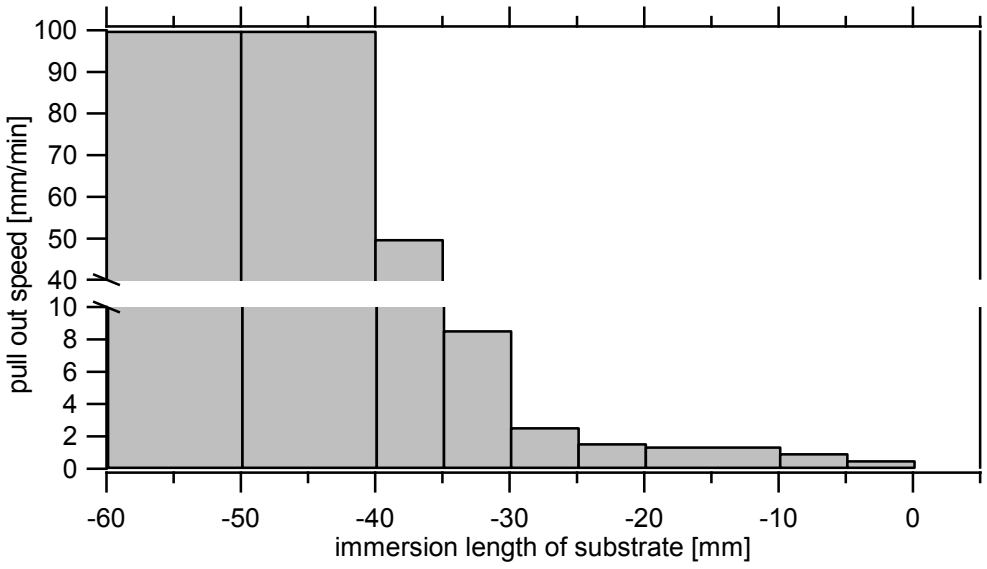

Figure S3: Histogram of the used withdrawal ramp. The substrate is immersed 60 mm and afterward pulled out with decreasing speed.

SI 4: Evaluation of the mean interparticle distance from the radial distribution function

To calculate the average interparticle distance between the assembled gold cores a radial distribution function was generated using a SEM image with 1633 particles on an area of 80 μm^2. The average center-to-center distance of the gold cores is 233 nm as determined from the first maximum of the radial distribution function. From the five distinct RDF peaks the high structural quality of the monolayer can be evaluated.

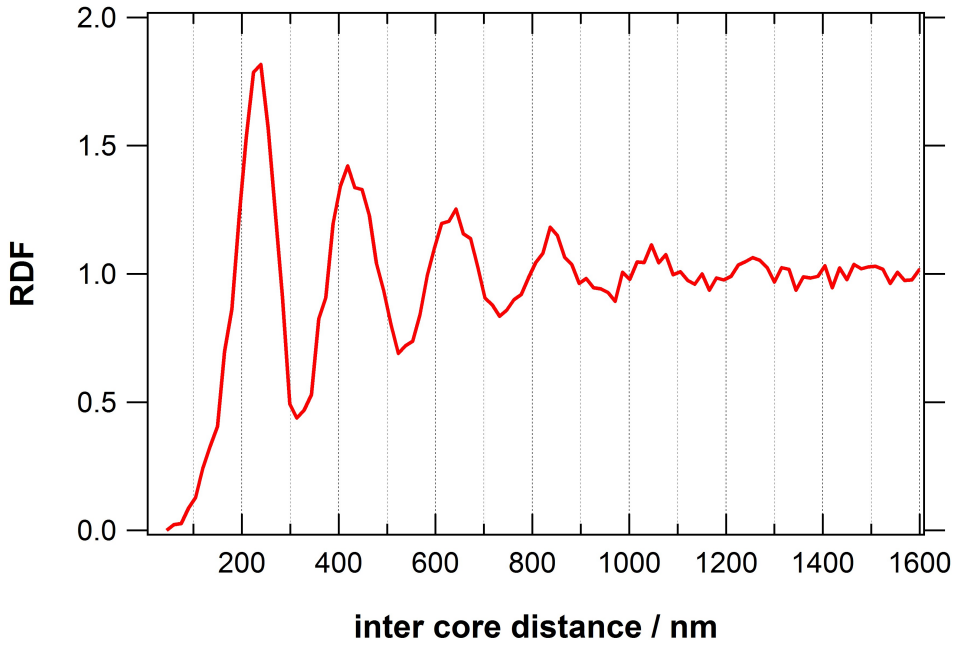

Figure S4: Radial distribution function of Au-core/PNIPAM-shell particle monolayer assembled on a glass substrate.

SI 5: Evaluation of the volume fraction of gold throughout the gradient

Between position **B** and **G** of Figure S5A the volume fraction is in the same range and the first position where an increase in the volume fraction is visible is at position **H**. This is related to the detection of a stronger UV-vis signal and less noisy spectra. Figure S5B shows the amount of non-spherical objects for the positions on the substrate. We assumed particles with a circularity higher than 0.85 as spherical. At least 1400 particles were investigated per sample position. The number of non-spherical particles is increasing along the gradient and is 12% for the longest immersion times at position **P**.

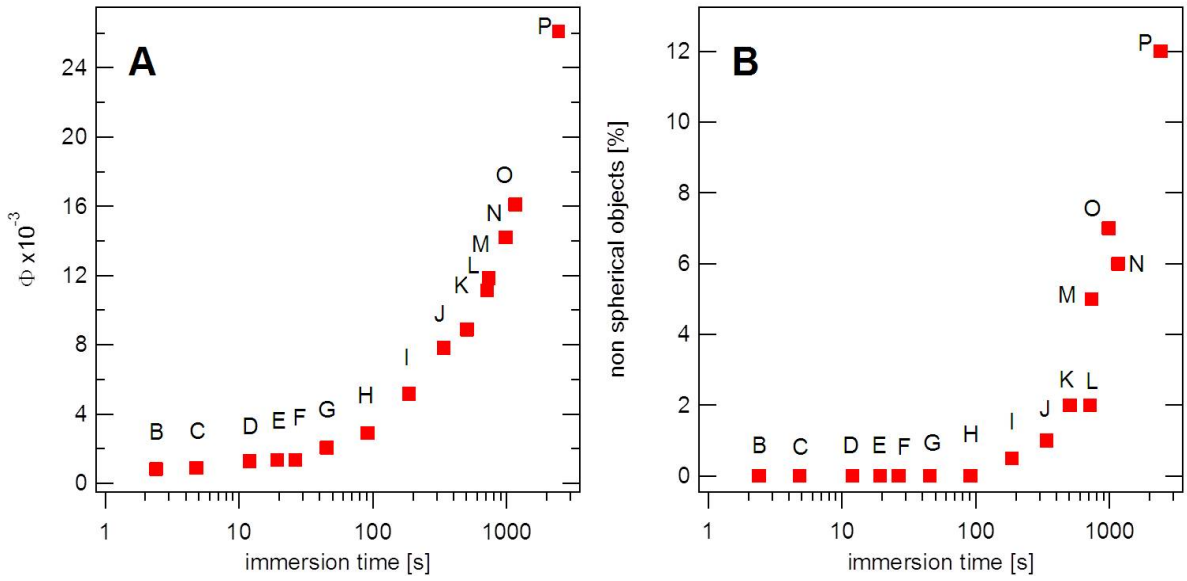

Figure S5: (A) Increasing volume fraction of the gold cores in a hypothetical layer of the same height as the gold core diameter. (B) Amount of none-spherical objects (circularity less than 0.85) for increasing exposure time in the growth solution.

SI 6: Quantitative description of the red shift of the LSPR for different particle diameter by an allometric power law according to Mie theory

To describe the shift of the plasmon resonance λ_{LSPR} for increasing particle diameter in different surroundings of refractive index n, we applied the following allometric power law:

$$\lambda_{LSPR}(d) = k\, d^{\,a} + c \qquad \text{(S1)}$$

with k as amplitude, a as scaling exponent, c as offset constant, and R^2 as coefficient of determination. Table S1 summarizes the coefficients used in Figure 4.

Table S1: Summary of coefficients used to determine the LSPR shifts by Mie theory.

n	k / nm$^{(1-a)}$	a	c / nm	R^2
1.52	0.0019	2.30	537.6	0.998
1.46	0.0115	1.83	531.9	0.998
1.35	0.0005	2.25	525.1	0.998
1.00	0.0001	2.63	505.4	0.995

SI 7: Determination of the average surrounding refractive index from Mie theory

To obtain the average surrounding refractive index from the plasmonic resonance position at specific particle diameter, we made a parabolic fit to the LSPR position (equation, errors, and coefficient of determination are given in the inset of Figure S7), which we determined from Mie theory at different surrounding refractive indices.

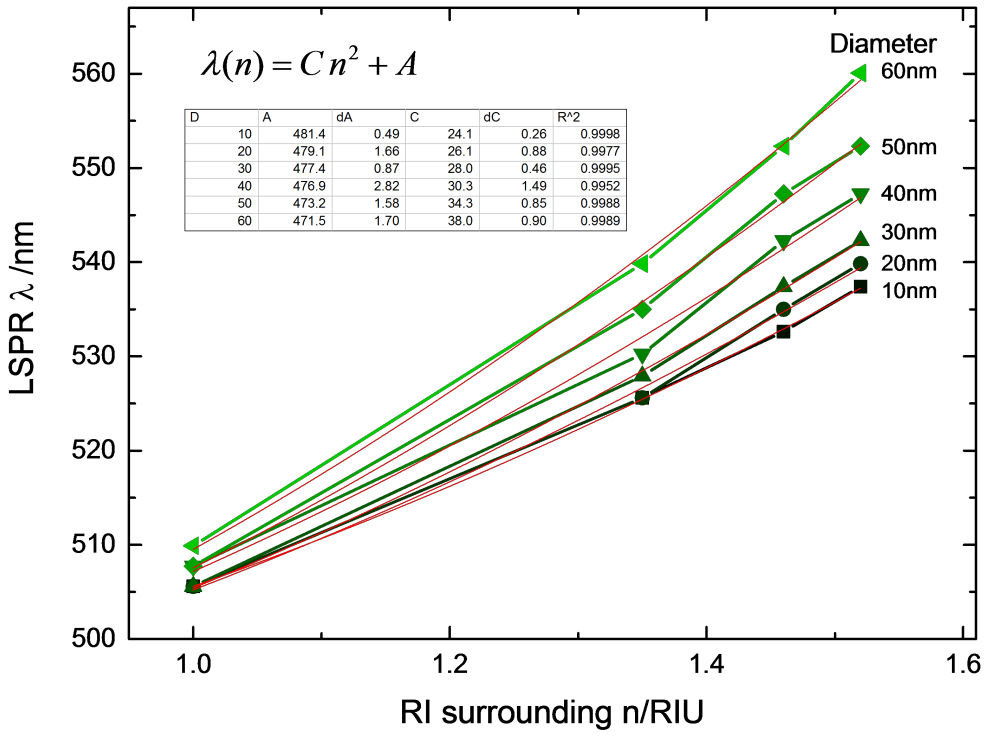

Figure S7: LSPR red shift *versus* surrounding refractive index and parabolic fit (solid red lines) at different gold core diameter.

References

(1) Karg, M.; Jaber, S.; Hellweg, T.; Mulvaney, P. Surface Plasmon Spectroscopy of Gold–Poly-N-Isopropylacrylamide Core–Shell Particles. *Langmuir* **2011**, *27*, 820–827.